Deutsches Institut
für Kautschuktechnologie e.V.

DIK Preprints

Current topics from Rubber Technology

Manuscript intended for submission
to peer-reviewed journals

Preprint:	1
Date:	18th December 2018
Authors:	Oliver Gehrmann, Nils Hendrik Kröger, Maria Krause, Daniel Juhre
Title:	Dissipated energy as fatigue criterion for non-relaxing tensional loadings of non-crystallizing elastomers
Cited as:	submitted to Journal of Fatigue

Dissipated energy as fatigue criterion for non-relaxing tensional loadings of non-crystallizing elastomers?

Oliver Gehrmann[a,*], Nils Hendrik Kröger[a], Maria Krause[a], Daniel Juhre[b]

[a] *Deutsches Institut für Kautschuktechnologie e. V., Eupener Straße 33, 30519 Hanover, Germany*
[b] *Otto von Guericke University Magdeburg, Universitaetsplatz 2, 39106 Magdeburg, Germany*

Abstract

The influence of the minimum dynamic load on the mechanical fatigue properties of ethylene propylene diene rubber is investigated. Force controlled fatigue experiments with two different positive ratios of minimum and maximum tensile loads are compared with results based on fully relaxing loading conditions. These tests are conducted under exclusion of other factors influencing durability (e.g. specimen temperature, deformation rate) with an axisymmetric dumbbell specimen. In order to quantify the fatigue influence of the crack initiation on the dumbbell's parting line, fully relaxing dumbbell tests are compared with fully relaxing tests using a shear specimen with internal crack initiation. A minor durability reducing effect resulting from the crack initiations at the dumbbell's parting line can be measured. Various end-of-life predictors are applied on the experimental database. The recently often as promising end-of-life predictor discussed dissipated energy density shows disappointing properties compared to a standard predictor like elastic energy density.

Keywords: R-Ratio, Dissipated Energy, Non-crystallizing rubber, Fatigue testing, EPDM Rubber

1. Introduction

The importance of quick and accurate end-of-life prediction is still evident. One established way of estimating fatigue life where only the end-of-life is of interest, is a procedure developed by August Wöhler [1]. In that procedure, a mechanical parameter (the fatigue criterion) is required that unites the major causes for the end-of-life of test pieces and components to obtain an accurate end-of-life prediction.
The challenge in developing such a criterion is the large number of factors influencing durability (for a summary see Mars [2]). An even larger number of criteria can be found in the literature. An overview of approaches for predicting the fatigue life of rubber is given by Mars [3]. A criterion able to account for all the known factors influencing end-of-life of rubber is, by the knowledge of the authors, not yet discovered.
Recently the dissipated energy density has drawn the attention of researchers with its promising prediction results for varying types of loading, elastomers and compound compositions as discussed in the following section. In this study the ability of the dissipated energy density as an end-of-life predictor for a non-relaxing loaded synthetic polymer is compared with standard end-of-life predictors.

2. State of the Art - R-Ratio focused

In general, the effect of minimum load on the fatigue behavior of rubber like materials has been extensively investigated. Taking a closer look, one ascertains that the majority of these investigations were carried out on natural rubber based compounds. The first known study of natural rubber under non-relaxing cyclic

*Corresponding author
Email address: Oliver.Gehrmann@DIKautschuk.de (Oliver Gehrmann)

loading have been done by Cadwell [4]. Since than, many more studies followed on the life extending effect of the minimum load for natural rubber and to its, with that effect connected, ability of forming crystals under high tension (e.g. [5, 6, 7, 8, 9, 10, 11]). Only little attention has been dedicated to the effect of minimum load on the fatigue behavior on rubbery materials that are not able to form a significant amount of crystals under high tension. The to the authors only known studies to these non-crystallizing elastomers exposed to non-relaxing cyclic loadings are published by Abraham et al. [12] for ethylene propylene diene rubber (EPDM) and Poisson [13] for polychloroprene rubber (CR). Whereby Poisson mentions a possible strain induced crystallization of the investigations of CR as an explanation for the observed behaviors. The specimen temperature, deformation rate and specimen storage played a minor part in the investigations of Abraham.
Poisson applies the locally evaluated dissipated energy with success on a variation of non-proportional multiaxial loadings. Moreover, the dissipated energy shows promising predictions in the few existing publications [14, 15, 16, 17, 18]. Marco even demonstrates the ability of the dissipated energy to predict the correct end-of-life for varying filler content and type [19].

3. Experiments

Material. The EPDM mixture, see Table 1, is prepared on a 1.5 liter mixer and admixed with the crosslinking agent and catalysts at the roller. The samples are compression molded at 160°C for 28 min.

Ingredients	EPDM	Carbon black N-347	Oil	Zinc oxid	Stearic acid	Sulphur	TBBS	TBzTD
Phr	100	50	40	4	2	0.7	1	3.5

Table 1: Recipe of the investigated EPDM mixture

Specimen. The specimen to investigate the fatigue behavior of the non-crystallizing EPDM is the axisymmetric dumbbell specimen shown in Figure 1. The analysis of the crack origin reveals that approximately half of the cracks initiate at the mold partition line (see Figure 3). The mold partition line is not an inhomogeneity which is not considered as a material specific property compared to inhomogeneities originating from filler particles. To obtain an estimate of the influence of the partition line based crack initiations a shear specimen shown in Figure 2 is used as a reference. Due to the shape of the shear specimen's metal insert the cracks initiate in the inner volume. The specimens are tested on a hydraulic MTS 831 Elastomer Test System.

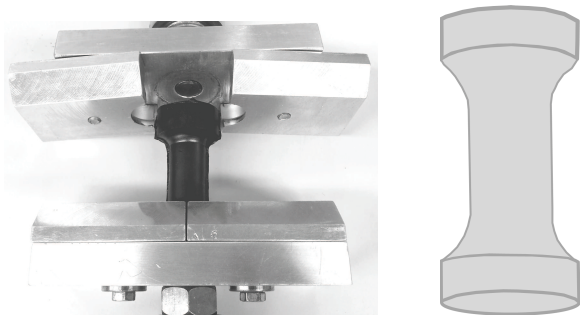

Figure 1: The axis-symmetric dumbbell specimen. The specimen is shown half attached in its fixture (left) and as a schematic sketch (right).

Figure 2: The shear specimen with typical crack initiations (highlighted in red) in the volume of the sliced specimen after one-sided cyclic shear load.

Test protocol. All tests are load controlled. The ratio between minimum load and maximum load, the R-ratio, is varied for the dumbbell specimen. The later comparison of the fully-relaxing dumbbell tests with the shear tests serves as a measure for the influence of the mold partition line. These two tests can be compared since no measurable difference in durability can be found between the uniaxial and simple shear deformation mode (proven in [20]). Investigating a factor influencing fatigue it should be in general considered that it is necessary to reduce the effect of the other known influencing parameters as much as possible. Using this approach, the factor of interest can be isolated and analyzed. Therefore, the specimen surface temperature during cyclic loading is kept close to room temperature by using forced convection (see Table 2). The core temperature is measured to be maximal $\Delta T = 8°C$ warmer compared to the specimen's surface temperature. In order to eliminate a possible influence of the deformation rate the frequency is adjusted for each load level, based on the deformation rate at the specimen's hotspot (see Table 2). The hotspot is defined as the point of highest deformation in a load cycle and is determined with a Finite Element Simulation. Furthermore, for the complete test campaign all specimens are vulcanized from one batch and were tested within one month. The samples were stored at an ambient temperature of around 8°C to exclude aging and at the same time possible effects from defrosting.
The test protocol results in four Wöhler curves.

	Load [N]	Frequency [Hz]	R-ratio	Surface temperature [°C]
Dumbbell tests	130 ± 130	1.5	0.0	27
	110 ± 110	2.0		26
	90 ± 90	2.7		26
	230 ± 130	1.7	≈ 0.3	27
	210 ± 110	2.0		26
	190 ± 90	2.4		25
	330 ± 130	3.2	≈ 0.5	23
	310 ± 110	4.2		23
	290 ± 90	4.4		23
Shear tests	550 ± 550	1.5	0.0	24
	500 ± 500	1.7		23
	450 ± 450	1.9		23

Table 2: Test protocol with dynamic loads, corresponding frequency and R-ratio.

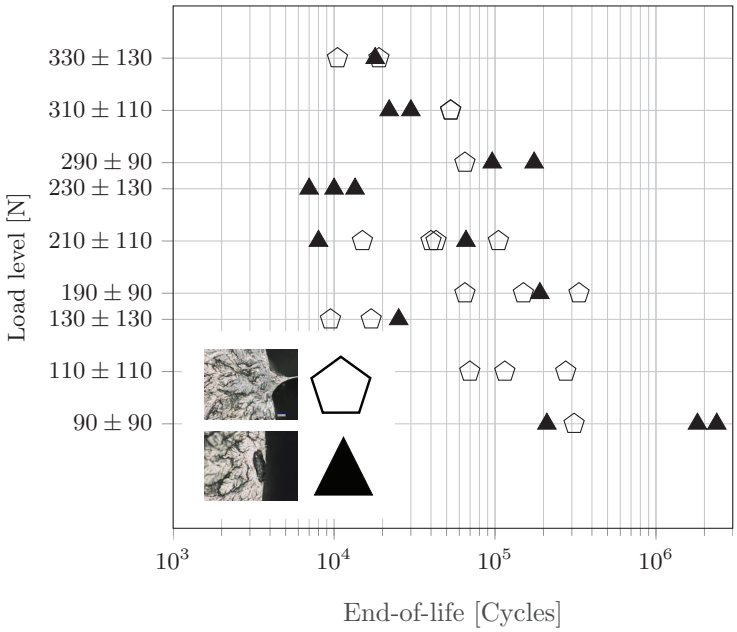

Figure 3: Cause for the crack initiation vs. end-of-life of the dumbbell specimen. Crack initiations at the mold partition line are symbolized with a pentagon ⬠ and crack initiations at a particle are symbolized with a triangle ▲.

Test data evaluation. Before making any statements about the behavior of the EPDM based material with increasing R-ratio, the test data are evaluated. The overall validity of the Wöhler curve database is verified by evaluating the global influence of the dumbbell specimen's position in the mold, the shear specimen's position in the test fixture, the positions and origins of the crack initiations on the end-of-life.
No correlation can be found between the cycles until end-of-life and the position in the mold for the dumbbell specimen (see Figure 4). The evaluated positions are chosen cause to the possible lower temperatures in the outer area of the mold compared to its center. Such a study is not required for the shear specimen since the corresponding mold has only one cavity.

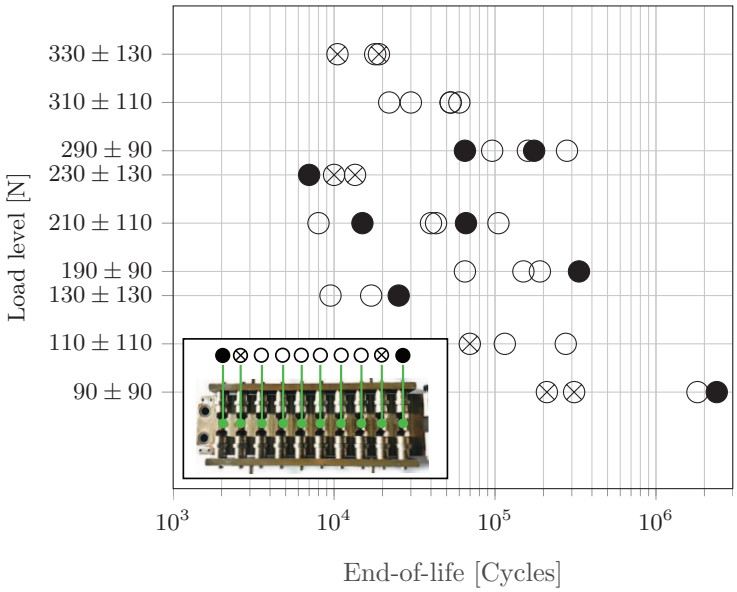

Figure 4: Position of the dumbbell specimen in the vulcanisation mold vs. End-of-life.

The study of the position and origin of the crack initiation reveals no general influence on the end-of-life of these parameters. As expected, a significant larger amount of cracks initiate close to the radius for the dumbbell specimen. The area of maximal deformation, the hotspot, is close to that area.
Tests are considered as invalid if cracks initiate at the fixture (dumbbell specimen) or resulting from failure of the bonding system (shear specimen). Invalid data points are removed from the database.

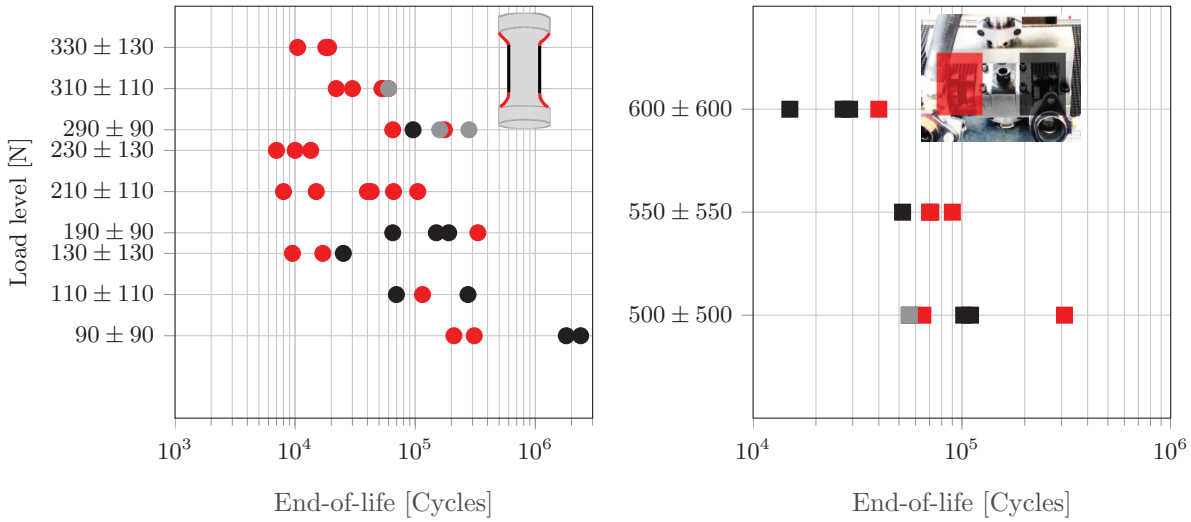

Figure 5: Position of crack initiation vs. end-of-life. Markers colored in gray symbolize crack initiations caused by the clamping of the sample or caused by a fail of the bonding system. The ordinate shows the load level in Newton [N].

For the remaining data points the medians are calculated. To be able to compare the shear tests with the dumbbell tests, the medians of the shear tests are additionally shifted based on the sudden death testing

principal (e.g. [21]). It means, that the complete test is stopped if one of two in parallel tested specimen has failed. In general, a specimen is considered as failed if the dynamic stiffness drop cannot anymore be associated with the material specific viscoelastic stiffness drop. Crack lengths of 2 mm to 5 mm can be found at the end-of-life for the used specimens, based on that approach. The approach is motivated by the work of Ostoja Kuczynksi et al. [22]. The calculations of the means and the consideration of the sudden death testing for shear specimen are based on the Weibull distribution [23].

4. Simulation

The criteria from Table 3 are chosen to be investigated as possible end-of-life predictors. Next to frequently applied criteria such as the maximum principal stress, strain and the elastic energy density the dissipated energy density is deployed, too.

Max(Criterion)	ΔCriterion	Description
ε_1	$\Delta\varepsilon_1$	maximum principal nominal strain
σ_1	$\Delta\sigma_1$	maximum principal Cauchy Stress
Energies		
$\Psi_{el.Tensor}$		elastic energy density, tensor based
$\Psi_{d.Tensor}$		dissipated energy density, tensor based
$\Psi_{d.MaxRD}$		dissipated energy density, calculated from the maximal loaded representative direction

Table 3: Overview over the chosen criteria.

The schematic sketch shown in Figure 6 visualizes the difference between max(Criterion) and ΔCriterion from Table 3.

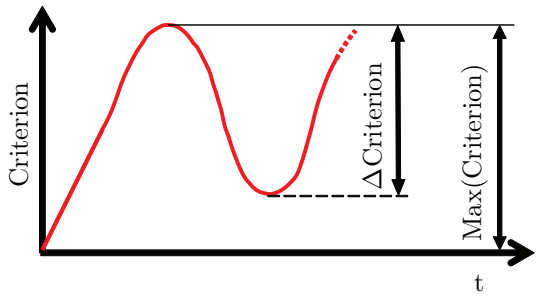

Figure 6: Explaination of Max(Criterion) and ΔCriterion.

Finite element analysis based on sophisticated material models are necessary, to be able to determine the chosen criteria at the hotspots of the specimens. The for the applied loadings optimized finite element meshes are shown in Figure 7. The used material model is the Model of Rubber Phenomenology (MORPH) which is able to describe the non-linear behavior, softening, moderate permanent set and hysteresis of a filled rubber material under large deformations [24]. This complex material model is implemented via the concept of the representative directions [25] and allows therefore the evaluation of single representative directions. The criterion $\Psi_{d.MaxRD}$ uses only the stress-strain data from the maximal loaded direction.

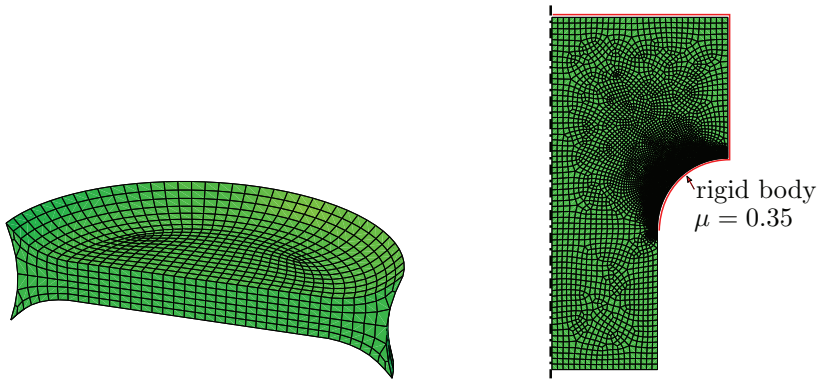

Figure 7: FE-Models of the Dumbbell and Shear specimen.

The determination of the MORPH material parameters uses the dumbbell finite element model from Figure 7 and directly the fatigue test's force-displacement data. The experimental force-displacement data are extracted at the half end-of-life, because for the majority of the specimen's lifetime it is loaded under these conditions. Based on the determined parameters, a very precise match of the numerical and experimental data can be observed in Figure 8. The numerical data in Figure 8 show the 10^{th} loading cycle. This shown force-displacement characteristic is therefore stress softening independent. The shear specimen is not included in the procedure of parameter identification. Even so, the match between the numerical and experimental force-displacement data has the same accuracy level as shown in Figure 8 for the dumbbell specimen.

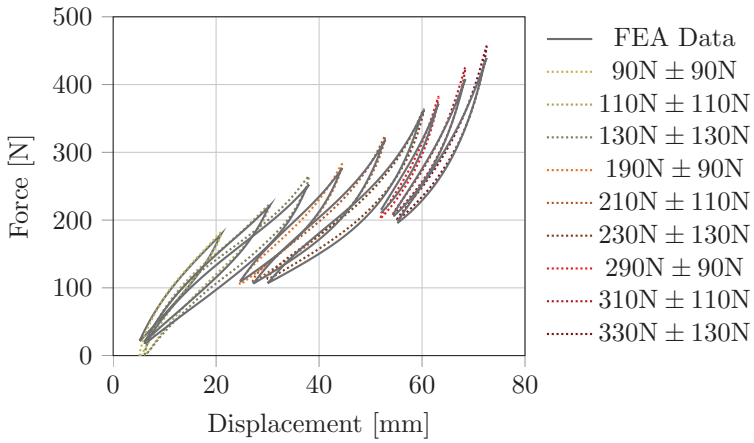

Figure 8: Experimental force-displacement-data superimposed with the FEA data.

Figure 9 shows the basic procedure of calculating the different types of energies from a hysteresis loop in a stress-strain plot.

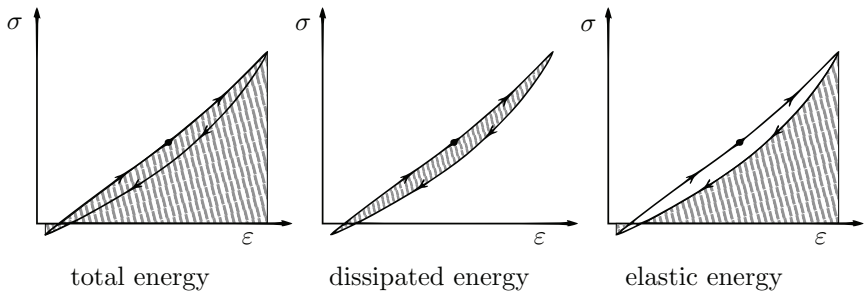

Figure 9: A principal sketch of the determination of the total, dissipated and elastic energy in a stress-strain plot.

The implemented method uses the strain energy history over one load cycle. That strain energy density originated from the full stress and strain tensor as defined in Equation 1:

$$\Psi = \int \underline{\underline{\sigma}} : \partial \underline{\underline{\varepsilon}} \tag{1}$$

The local stress and strain tensors are derived by from Finite Element Simulations. They are evaluated at every integration point. Therefore the strain energy density is a locally for every integration point calculated quantity.

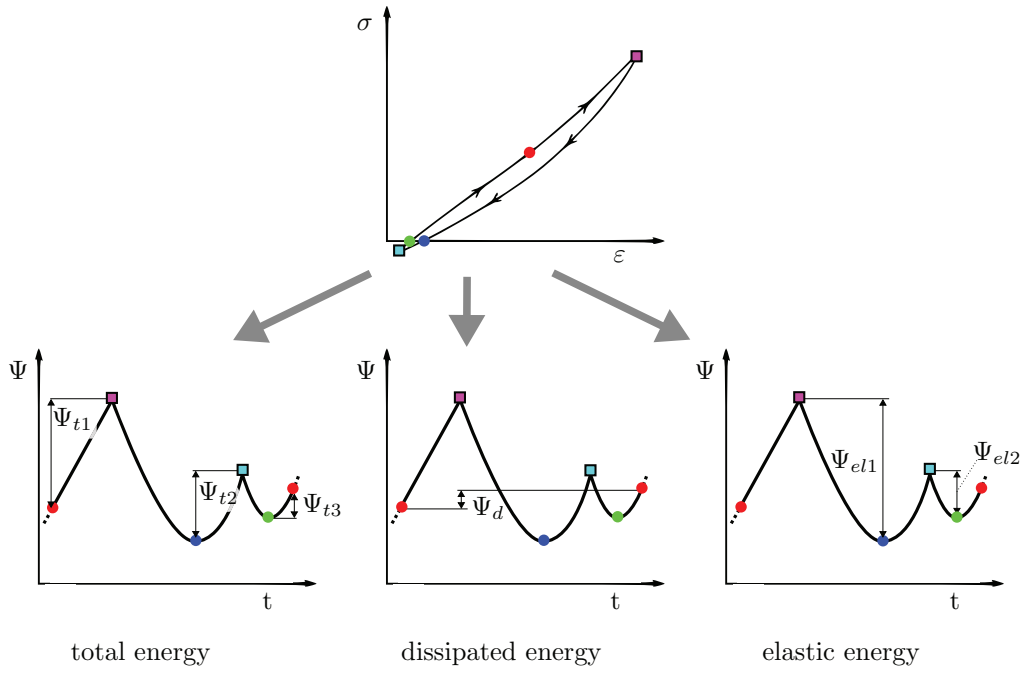

Figure 10: The determination of the total, dissipated and elastic energy from the numerical data.

The terms of the sum of the total Ψ_{ti} and elastic energy density Ψ_{eli} in the strain energy density history are shown in Figure 10. The dissipated energy Ψ_d arises from the difference in strain energy density at the start and end of a load cycle.
Figure 11 shows all Wöhler curves based on the maximum principal nominal strain. For the judgement of

an end-of-life criterion the data points for each load level are replaced with their means. Only these means are fitted by a power function as shown in Figure 11. The coefficient of determination R^2 serves as a scalar measure for the quality on the investigated criterion as an end-of-life predictor. Fitting only the mean values enables theoretically an $R^2 = 1$ for the optimum end-of-life predictor. The natural scattering in the number of cycles to end-of-life is eliminated in the statement about the criterion's quality. The 95% confidence limits are given for each mean value.

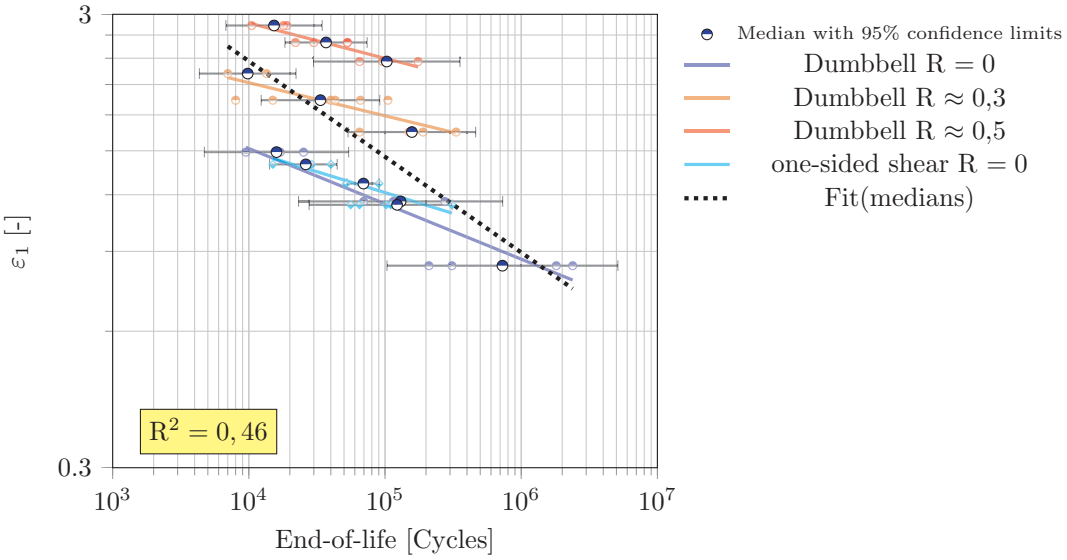

Figure 11: Superposition of the Wöhler curves for ε_1 with coefficient of determination based on the logarithmic medians only.

By using maximum principal nominal strain as a possible end-of-life predictor a strong reinforcement effect regarding the end-of-life is visible (see Figure 12, left). The opposite is statable by using the peak to peak strains $\Delta\varepsilon_1$ (see Figure 12, right).

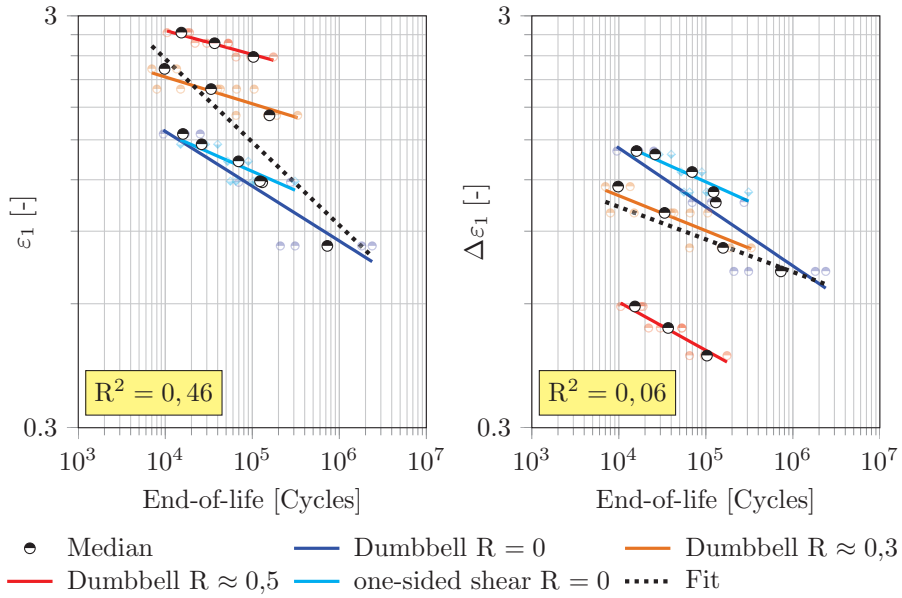

Figure 12: Superposition of the Wöhler curves based on ε_1 and $\Delta\varepsilon_1$.

A quite similar reinforcing effect, compared to ε_1, can be found for the criterion of the maximum value of the principal Cauchy stress σ_1 in Figure 13. In contrast to the complete rearrangement of the Wöhler curves when switching from ε_1 to $\Delta\varepsilon_1$, the order of the Wöhler curves stays untouched between σ_1 and $\Delta\sigma_1$.

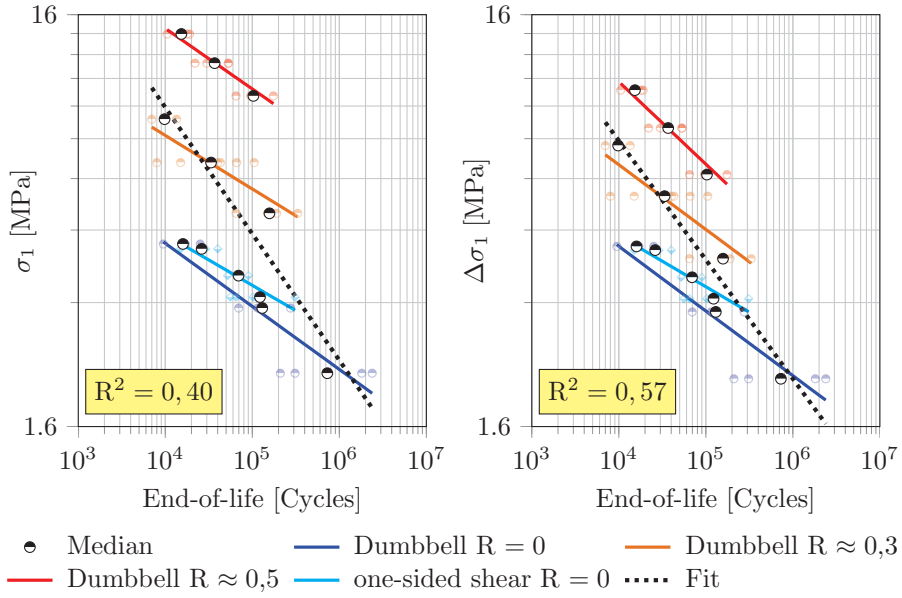

Figure 13: Superposition of the Wöhler curves based on σ_1 and $\Delta\sigma_1$.

Plotting the peak to peak strains $\Delta\varepsilon_1$ over its corresponding mean strains reveals the, already in Figure 12 right visible, significant decrease of bearable number of cycles until failure (see Figure 14, left). Iso-durability lines connect points with equal durabilities.

Opposed to this, an increasing lifetime with increasing mean stress becomes obvious by the positive slope of the iso-durability curves in the $\Delta\sigma_1$ over mean stress diagram (see Figure 14, right).

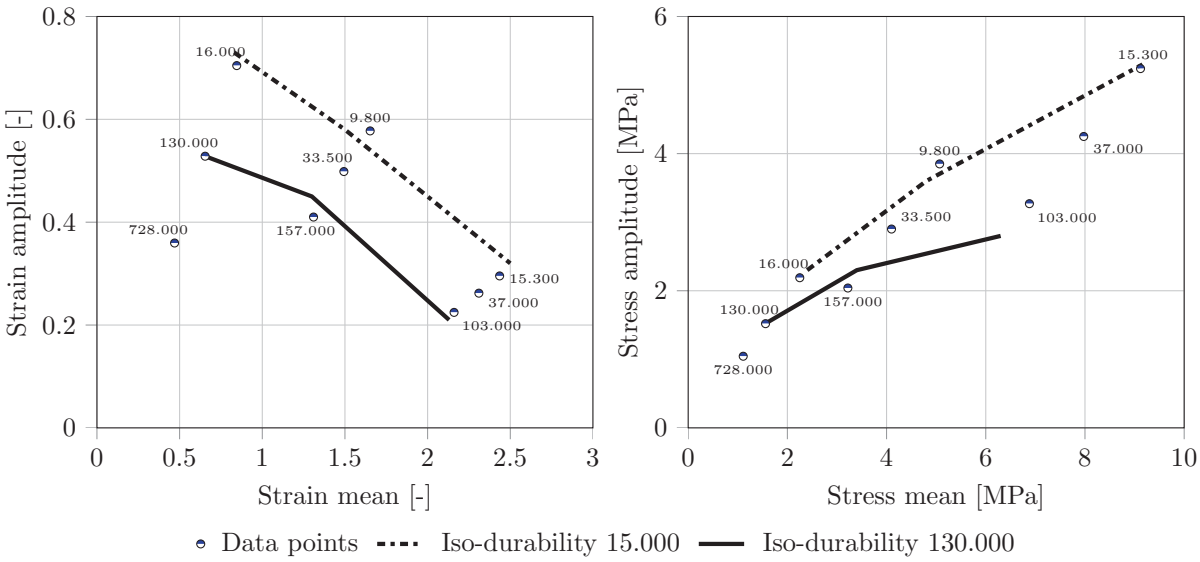

Figure 14: Haigh-diagram based on the maximum principal nominal strains and maximum principal Cauchy stress.

When applying the elastic strain energy density the Wöhler curves are shifted close to each other, correlating to the results of Abraham [12]. The coefficient of determination confirms that visual impression.

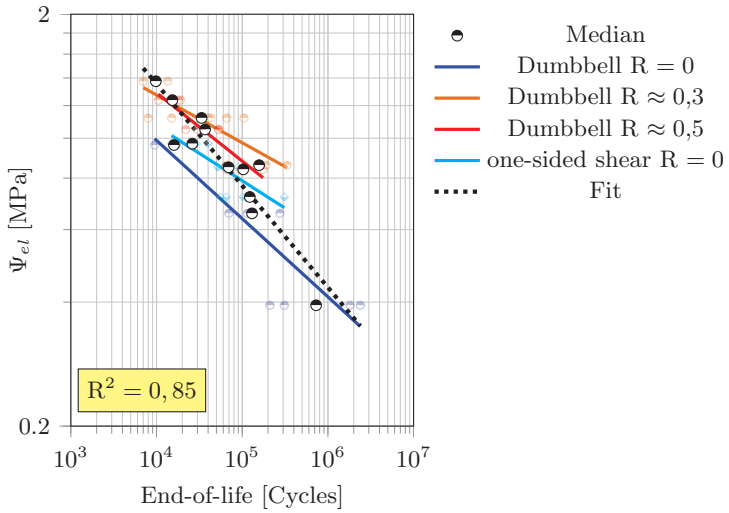

Figure 15: Superposition of the Wöhler curves based on Ψ_{el}.

The dissipated energy shows unsatisfactory results for both versions as indicated by R^2 (see Figure 16).

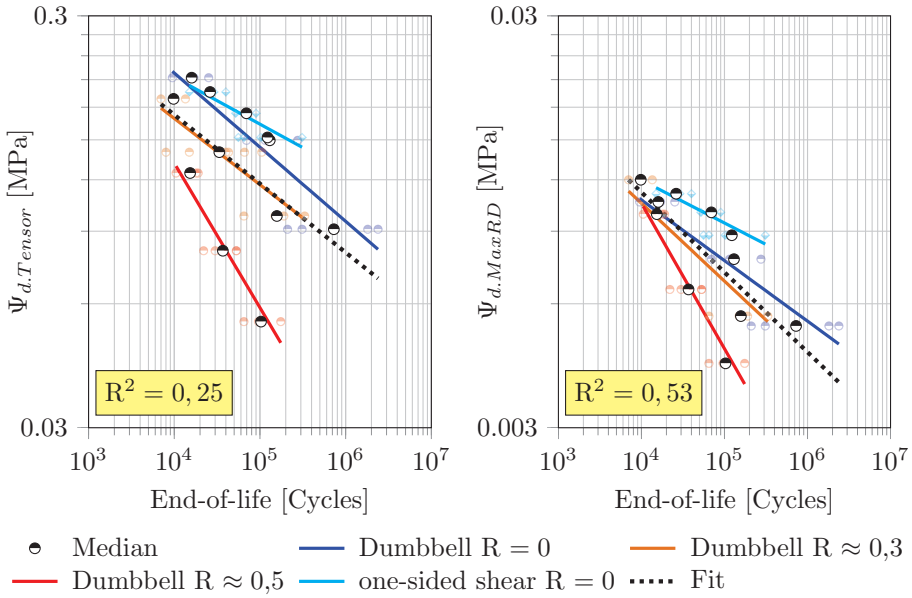

Figure 16: Superposition of the Wöhler curves based on $\Psi_{d.Tensor}$ and $\Psi_{d.MaxRD}$.

5. Discussion

Summing up the results of the investigated criteria, the elastic strain energy density Ψ_{el} shows the best level of Wöhler curve superposition, so the best quality as an end-of-life predictor for the used loadings and material (see Figure 17).

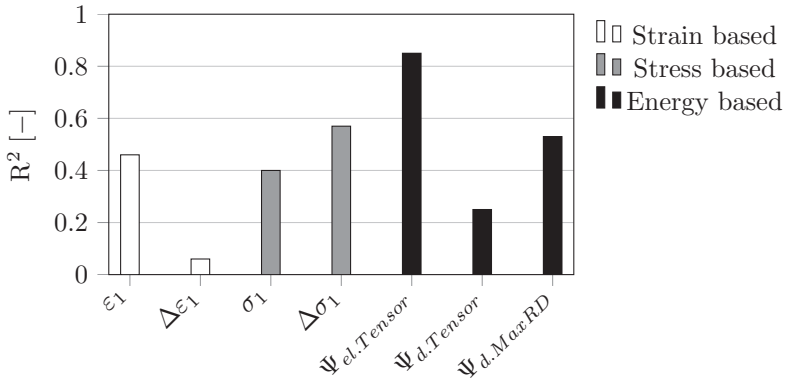

Figure 17: Coefficient of determinations based on the complete Wöhler curve database.

It is conceivable to implement the information from Figure 14, left and right, in $\Delta\varepsilon_1$ and $\Delta\sigma_1$, respectively. The remaining disadvantage would be that different strain states stay unconsidered in these, on maximum principal values based, criteria. The strain state has a significant influence on the fatigue behavior of elastomers [26].
Both versions of the fatigue criterion dissipated energy density show unsuitable properties for the R-ratio variation in combination with the non-crystallizing EPDM rubber. That combination of loadings and material might be a limit for the otherwise promising quality of that criterion in the known literature.

The fully-relaxing simple shear tests serve as reference for the fully-relaxing dumbbell tests. Since the different strain states of these two specimen do not influence the fatigue. The comparison of them provides information about the influence of the crack initiation at the dumbbells parting line on the fatigue. The one-sided shear tests tend to an increased lifetime (see all Wöhler curve plots in the previous section). That shift is assumed to be caused by the crack initiations at the dumbbells parting line.

6. Acknowledgment

The authors would like to thank the following companies for their financial support: BOGE Elastmetall GmbH, Continental Reifen GmbH, ContiTech AG, Freudenberg New Technologies, Henniges Automotive, Veritas AG, Vibracoustic.

References

[1] A. Wöhler, Über die festigkeitsversuche mit eisen und stahl., Zeitschrift für Bauwesen (Vol. 20) (1870) S. 73–106.
[2] W. V. Mars, A. Fatemi, Factors that affect the fatigue life of rubber: A literature survey, Rubber Chemistry and Technology (77) (2004) 391–412.
[3] W. V. Mars, A. Fatemi, A literature survey on fatigue analysis approaches for rubber, International Journal of Fatigue (24) (2001) 949–961.
[4] S. M. Cadwell, R. A. Merrill, C. M. Sloman, F. L. Yost, Dynamic fatigue life of rubber, Rubber Chemistry and Technology (13) (1940) 304–315.
[5] E. Ostoja-Kuczynski, P. Charrier, E. Verron, L. Gornet, G. Marckmann, Influence of mean stress and mean strain on fatigue life of carbon black filled natural rubber, Constitutive Models for Rubber IV (4) (2005) 15–22.
[6] J. B. Le Cam, E. Verron, B. Huneau, Description of fatigue damage in carbon black filled natural rubber, Fatigue & Fracture of Engineering Materials & Structures (31) (2008) 1031–1038.
[7] N. Andre, G. Gailletaud, R. Piques, Haigh diagram for fatigue crack initiation prediction of natural rubber components, Kautschuk und Gummi Kunststoffe (52) (1999) 120–123.
[8] S. Toki, T. Fujimaki, M. Okuyama, Strain-induced crystallization of natural rubber as detected real-time by wide-angle x-ray diffraction technique, Polymer (41) (1999) 5423–5429.
[9] Lee, H. J, W. D. Kim, B. I. Choi, C. S. Woo, J. Y. Kim, S. K. Koh, Fatigue life prediction of automotive rubber engine mount., International Journal of Fatigue (26) (2004) 553–560.
[10] Shangguan, W. B, X. Duan, T. Liu, Prediction fatigue life of rubber mounts using stress-based damage indexes., Journal of Materials: Design and applications (231) (2015) 657–673.
[11] H. Oshima, Y. Aono, H. Noguchi, Fatigue characteristics of vulcanized natural rubber for automotive engine mounting, Key Engineering Materials (353-358) (2007) 178–181.
[12] F. Abraham, T. Alshuth, S. Jerrams, The effect of minimum stress and stress amplitude on the fatigue life of non strain crystallising elastomers, Materials and Design (26) (2004) 239–245.
[13] J.-L. Poisson, F. Lacroix, S. Meo, G. Berton, N. Ranganathan, Biaxial fatigue behavior of a polychloroprene rubber, International Journal of Fatigue (33) (2011) 1151–1157.
[14] T. Brüger, M. Rabkin, U. Weltin, Hysteresis area calculated from a dynamic material model: A new damage parameter for lifetime estimations?, Constitutive Models for Rubber IV 2005 (2005) 83–88.
[15] V. Le Saux, Y. Marco, S. Calloch, C. Doudard, P. Charrier, Fast evaluation of the fatigue lifetime of rubber-like materials based on a heat build-up protocol and micro-tomography measurements, International Journal of Fatigue (32) (2010) 1582–1590.
[16] V. Le Saux, Y. Marco, S. Calloch, C. Doudard, P. Charrier, An energetic criterion for the fatigue of rubbers: an approach based on a heat build-up protocol and mirco-tomography measurements, Procedia Engineering (2) (2010) 949–958.
[17] J.-L. Poisson, S. Meo, F. Lacroix, G. Berton, M. Hosseini, N. Ranganathan, Comparison of fatigue criteria under proportional and non proportional multiaxial loading., Rubber Chemistry and Technology (91(2)) (2018) 320–338.
[18] F. Lacroix, S. Meo, G. Berton, F. Chalon, A. Tougui, N. Ranganathan, A local criterion for fatigue crack initiation on chloroprene rubber: approach in dissipation, Constitutive models of rubber IV. (2005) 77–82.
[19] Y. Marco, I. Masquelier, V. Le Saux, P. Charrier, Fast prediction of the woehler curve from thermal measurements for a wide range of nr and sbr compounds, Rubber Chemistry and Technology 90 (3) (2017) 487–507.
[20] E. Ostoja-Kuczynski, Comportement en fatigue des élastomères: application aux structures antivibratoires pourlautomobile. dissertation, Ecole Centrale de Nantes, Université de Nantes (2005).
[21] W. Nelson, Accelerated testing, A JOHN WILEY & SONS (1990).
[22] E. Ostoja Kuczynski, P. Charrier, E. Verron, G. Marckmann, Crack initiation in filled natural rubber: experimental database and marcoscopic observations, Constitutive models of rubber III (2003) 41–47.
[23] W. Weibull, A statistical theory of the strength of materials, Generalstabens litografiska anstalts förlag (1939).
[24] D. Besdo, J. Ihlemann, A phenomenological constitutive model for rubberlike materials and its numerical applications, International Journal of Plasticity (19) (2003) 1019–1036.

[25] M. Freund, J. Ihlemann, Generalization of one-dimensional material models for the finite element method., ZAMM J. Appl. Math. Mech. (90) (2010) 399—-417.
[26] B. J. Roberts, J. B. Benzies, The relationship between uniaxial and equibiaxial fatigue in gum and carbon black filled vulcanizates, Proceedings of Rubbercon (1977) 1–13.